jbc The Journal of Biological Chemistry
AFFINITY SITES
ASBMB American Society for Biochemistry and Molecular Biology

Signal Transduction:

Analysis of Ca2+ Signaling Motifs That Regulate Proton Signaling through the Na+/H+ Exchanger NHX-7 during a Rhythmic Behavior in Caenorhabditis elegans

Erik Allman, Korrie Waters, Sarah Ackroyd and Keith Nehrke

J. Biol. Chem. 2013, 288:5886-5895.
doi: 10.1074/jbc.M112.434852 originally published online January 14, 2013

Access the most updated version of this article at doi: 10.1074/jbc.M112.434852

Find articles, minireviews, Reflections and Classics on similar topics on the JBC Affinity Sites.

Alerts:
- When this article is cited
- When a correction for this article is posted

Click here to choose from all of JBC's e-mail alerts

Supplemental material:
http://www.jbc.org/content/suppl/2013/01/14/M112.434852.DC1.html

This article cites 70 references, 38 of which can be accessed free at
http://www.jbc.org/content/288/8/5886.full.html#ref-list-1

Downloaded from http://www.jbc.org/ at University of Rochester on June 17, 2013

THE JOURNAL OF BIOLOGICAL CHEMISTRY VOL. 288, NO. 8, pp. 5886–5895, February 22, 2013
© 2013 by The American Society for Biochemistry and Molecular Biology, Inc. Published in the U.S.A.

Analysis of Ca^{2+} Signaling Motifs That Regulate Proton Signaling through the Na^+/H^+ Exchanger NHX-7 during a Rhythmic Behavior in *Caenorhabditis elegans*[*] [S]

Received for publication, November 8, 2012, and in revised form, December 20, 2012 Published, JBC Papers in Press, January 14, 2013, DOI 10.1074/jbc.M112.434852

Erik Allman[‡], **Korrie Waters**[§], **Sarah Ackroyd**[¶], **and Keith Nehrke**[‡¶1]

From the Departments of [‡]*Pharmacology and Physiology and* [¶]*Medicine, University of Rochester School of Medicine and Dentistry, Rochester, New York 14642 and the* [§]*Department of Family Medicine, Ohio University, Athens, Ohio 45701*

Background: Ca^{2+} oscillations stimulate rhythmic proton signaling by Na^+/H^+ exchanger NHX-7 in *C. elegans*.
Results: The contribution of individual regulatory motifs to NHX-7 activity was defined by *in vivo* structure-function analysis.
Conclusion: NHX-7 activity is regulated by both Ca^{2+} and pH, leading to robust but transient signaling.
Significance: Understanding the mechanisms that distinguish proton signaling from pH regulation is critical for dual-function membrane transporters.

Membrane proton transporters contribute to pH homeostasis but have also been shown to transmit information between cells in close proximity through regulated proton secretion. For example, the nematode intestinal Na^+/H^+ exchanger NHX-7 causes adjacent muscle cells to contract by transiently acidifying the extracellular space between the intestine and muscle. NHX-7 operates during a Ca^{2+}-dependent rhythmic behavior and contains several conserved motifs for regulation by Ca^{2+} input, including motifs for calmodulin and phosphatidylinositol 4,5-bisphosphate binding, protein kinase C- and calmodulin-dependent protein kinase type II phosphorylation, and a binding site for calcineurin homologous protein. Here, we tested the idea that Ca^{2+} input differentiates proton signaling from pH housekeeping activity. Each of these motifs was mutated, and their contribution to NHX-7 function was assessed. These functions included pH recovery from acidification in cells in culture expressing recombinant NHX-7, extracellular acidification measured during behavior in live moving worms, and muscle contraction strength as a result of this acidification. Our data suggest that multiple levels of Ca^{2+} input regulate NHX-7, whose transport capacity normally exceeds the minimum necessary to cause muscle contraction. Furthermore, extracellular acidification limits NHX-7 proton transport through feedback inhibition, likely to prevent metabolic acidosis from occurring. Our findings are consistent with an integrated network whereby both Ca^{2+} and pH contribute to proton signaling. Finally, our results obtained by expressing rat NHE1 in *Caenorhabditis elegans* suggest that a conserved mechanism of regulation may contribute to cell-cell communication or proton signaling by Na^+/H^+ exchangers in mammals.

pH homeostasis is vital for maintaining protein folding/function and cell volume and for facilitating the flow of ions and nutrients through various physiologically coupled mechanisms (for review, see Ref. 1). pH imbalance has been implicated in a number of human diseases, including renal tubular acidosis, osteoporosis, and mental retardation, as well as in the transformation and metastasis of cancer (2–4). Because pH regulation plays a ubiquitous role in cell physiology and is crucial to an organism's health, it is not surprising that a wide variety of acid-base transporters exist (1).

However, recent evidence suggests that protons themselves may have an additional role in signaling between cells. Several types of mammalian proton receptors have been identified, including a class of G-protein-coupled receptors (GPR4, OGR1, G2A, and TDAG8), adhesion the kinase Pyk2, and cation channels of the Na^+ channel/degenerin superfamily (ASIC1/DRASIC) (5–9). These receptors are found in the kidney, brain, and central nervous system and have long been implicated in the perception of pain associated with tissue acidosis (10, 11). Reductions in extracellular pH arise during the course of ischemia, epileptic seizures, and electrical stimulation in the brain, suggesting a potential role for these proton receptors in human disease (12–16). Therefore, local regulation of proton availability may have important physiologic and pathophysiologic consequences through signal transmission processes. Membrane transporters that regulate pH homeostasis may also have a role in directing localized transient proton signals as part of an intercellular communication cascade. If so, it will be important to determine what particular features of such proteins distinguish their basal activity (which contributes to maintaining pH) from their stimulated acute activity during cell signaling.

Caenorhabditis elegans is a genetic model organism in which protons have been recently shown to be actively secreted as an intercellular signaling molecule during a rhythmic behavior (17, 18). Defecation is an ultradian behavior that occurs with a frequency of ~45 s in well fed worms (19, 20). The defecation

* This work was supported by Ruth L. Kirschstein National Research Service Institutional Award GM068411 from the National Institutes of Health (to E. A.). This work was also supported by National Science Foundation Grant IOS0919848 (to K. N.).
[S] This article contains supplemental "Experimental Procedures," Fig. S1, and additional references.
[1] To whom correspondence should be addressed: Dept. of Medicine, University of Rochester Medical Center, 601 Elmwood Ave., Rochester, NY. Tel.: 585-275-7020; Fax: 585-442-9201; E-mail: keith_nehrke@urmc.rochester.edu.

Downloaded from http://www.jbc.org/ at University of Rochester on June 17, 2013

motor program (DMP)[2] is characterized by three consecutive sets of muscle contractions (21). The first set is a contraction of the posterior body wall muscles (pBoc). This is closely followed by a contraction of the anterior body wall muscles and then expulsion of the luminal contents. Genetic analyses have shown that intestinal cell-autonomous oscillatory Ca^{2+} signaling is central to the defecation pacemaker (22). The first motor step of the DMP, pBoc, depends on Ca^{2+} signals initiating in the posterior cells of the intestine (17, 18), whereas a subsequent wave of Ca^{2+} that propagates posterior-to-anterior is necessary for the coupling and timing of the remaining motor steps (23–25).

A role for proton signaling during the DMP emerged from reports indicating that increased Ca^{2+} caused protons to move from the intestinal lumen into the cytoplasm, resulting in intracellular acidification, and that this in turn triggered proton extrusion across the basolateral membrane via the Na^+/H^+ exchanger NHX-7 (17, 18). Proton secretion was found to be both necessary and sufficient to trigger pBoc. Mechanistically, extracellular acidification resulting from NHX-7 activity was found to provide proton substrates that bound directly to and activated a ligand-gated cation channel, PBO-5/6 (pH_{50} ~6.8), expressed on the muscle membrane. Activation of PBO-5/6 resulted in muscle depolarization and pBoc (17). This was the first example of protons and a Na^+/H^+ exchanger contributing to acute intercellular signaling.

Na^+/H^+ exchangers are a 12-transmembrane-spanning family of phosphoglycoproteins that contain a hydrophobic N-terminal region and a large cytoplasmic C-terminal tail. They exchange one extracellular Na^+ for one intracellular H^+ to regulate intracellular pH (pH_i) and to maintain Na^+ homeostasis (26). They facilitate adhesion, migration, proliferation, and volume regulation (27–32) and have been implicated in a number of human diseases, including epilepsy, mental retardation, and cancer metastasis, in addition to being a component of ischemia/reperfusion injury (2–4). Mammals have nine isoforms of Na^+/H^+ exchangers termed NHEs (33–40), whereas the nematode *C. elegans* likewise codes for nine isoforms termed NHXs (41). Although some of these isoforms are ubiquitously expressed (NHE1 (42) and NHX-4 (41)) in a "housekeeping" manner, others demonstrate a high degree of cell-specific expression, suggesting potentially unique modes of regulation and function.

The basal activity of these NHEs can be modulated via a cytoplasmic allosteric proton-binding site that enhances activity upon intracellular acidification (low pH_i) (43) as well as by various protein interactions with regulatory motifs located in the C-terminal tail (26). This intracellular tail has also been shown to be the site of regulation by protein kinases, and these regulatory events can be a more powerful determinant of activity than the overall expression level of a given transporter (44). One ubiquitous and well studied regulatory mechanism is that of second messenger Ca^{2+} signaling. NHE1 and NHE3 both respond to changes in Ca^{2+} through a number of mechanisms, including phosphorylation by Ca^{2+}/calmodulin-dependent protein kinase type II (CaMKII) and interactions with Ca^{2+}-binding proteins such as calmodulin (CaM), calcineurin homologous protein (CHP), and tescalin (reviewed in Refs. 26) and 45). Thus, Ca^{2+} has the ability to both positively and negatively regulate Na^+/H^+ exchange and can do so in an isoform- and cell-specific manner.

Here, we present the results of a structure-function analysis focused on deciphering if and how Ca^{2+} signaling regulates NHX-7. We used dynamic fluorescent pH imaging to measure NHX-7 activity both in cells in culture and in live moving worms, where we could assess behavioral output. We hereby describe a role for CaM- and phosphatidylinositol 4,5-bisphosphate (PIP_2)-binding motifs in activation of the exchanger. Although we were further able to demonstrate that CaM interacts directly with NHX-7, we also found that it impacts oscillatory Ca^{2+} signaling upstream of NHX-7. Finally, a potential role for CaMKII phosphorylation in limiting the extent of proton transport may relate to the observation that extracellular acidification provides feedback inhibition and likely prevents metabolic acidosis from occurring.

EXPERIMENTAL PROCEDURES

Strains—Standard nematode culture techniques were used (46). Strains containing *pbo-4(ok583)*X, *pbo-5(n2303)*V, and *pha-1(e2123ts)*III alleles were obtained from the *Caenorhabditis* Genetics Center (University of Minnesota) and the *C. elegans* Gene Knockout Consortium. Other strains used in this work are described in detail under supplemental Experimental Procedures."

Quantitative RT-PCR—Gene expression levels were assayed in first-strand cDNA samples using iQ™ SYBR® Green Supermix (Bio-Rad) and standard protocols for real-time PCR and normalized to both *pmp-3* and *cdc-42* using the following primer pairs: *nhx-7*, 5′-CAGTACACTTTGCGAGTCGCTTAT-3′ and 5′-AGTTTGATCGTAGAACCCTGGATG-3′; *pmp-3*, 5′-GTTCCCGTGTTCATCACTCAT-3′ and 5′-ACACCGTCGAGAAGCTGTAGA-3′; and *cdc-42*, 5′-CTGCTGGACAGGAAGATTACG-3′ and 5′-CTCGGACATTCTCGAATGAAG-3′.

Molecular Biology—Plasmid constructs were created by conventional restriction site-mediated cloning methods. Site-directed mutagenesis was used to introduce point mutants, and inverse PCR was used to create deletions. Specific details as to the construction of the plasmids can be found under supplemental "Experimental Procedures." A plasmid containing the extracellular pH sensor was a kind gift of Dr. L. Pablo Cid (Centro de Estudios Científicos, Valdivia, Chile) and has been described previously (47). All constructs were verified via DNA sequencing.

Contraction Measurements—pBoc strength and duration were determined post hoc from transmitted light videos by measuring the perimeter of late L4 worms in their maximally relaxed and contracted states. Worms in which the reference points were obscured by movement, in either assay, were excluded from analysis.

[2] The abbreviations used are: DMP, defecation motor program; pBoc, posterior body wall muscle contraction; NHE, mammalian Na^+/H^+ exchanger; NHX, *C. elegans* Na^+/H^+ exchanger; CaMKII, Ca^{2+}/calmodulin-dependent protein kinase type II; CaM, calmodulin; CHP, calcineurin homologous protein; PIP_2, phosphatidylinositol 4,5-bisphosphate; rNHE1, rat NHE1; CBD, CaM-binding domain; DIC, differential interference contrast.

ASBMB Downloaded from http://www.jbc.org/ at University of Rochester on June 17, 2013

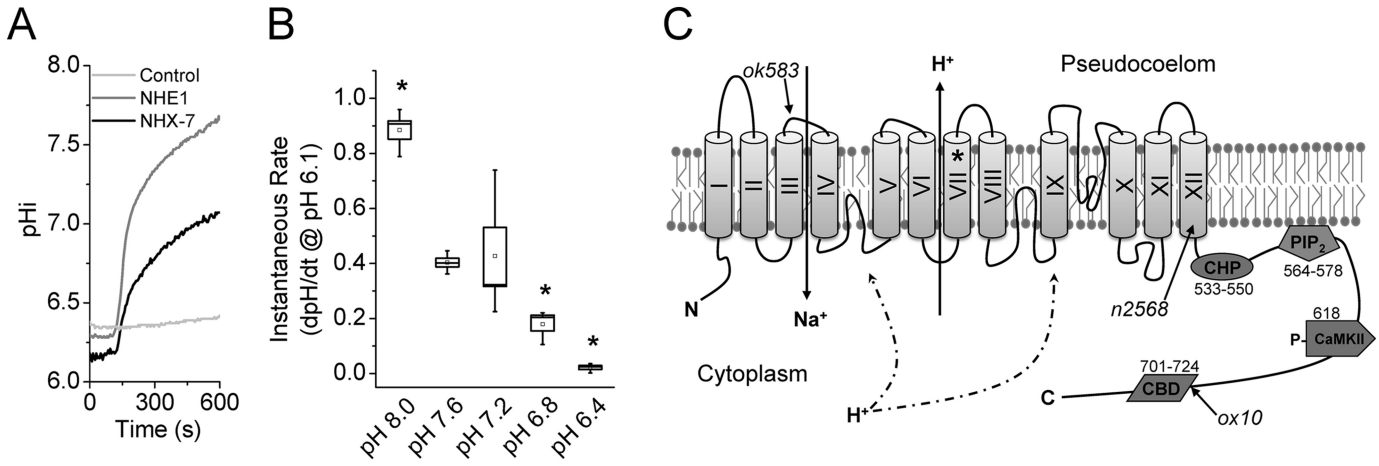

FIGURE 1. **Physiologic characterization of recombinant NHX-7 activity.** AP-1 cells, a CHO cell derivative that lacks NHE activity, were used for transient expression and fluorescence-based pH measurements of recombinant Na^+/H^+ activity. *A*, representative traces of Na^+-dependent pH recovery following acidification in cells expressing *C. elegans* NHX-7 or rat NHE1 as indicated. The negative control was the pcDNA3.1 vector alone. *B*, pH_e dependence of NHX-7. To calculate instantaneous recovery rate data, a best line fit equation was calculated for a 1-min window following the re-addition of Na^+ of a plot of dpH_i/dt *versus* pH and extrapolated to pH 6.1. Each data point represents three to four replicate experiments (>10 cells per experiment). The mean and median are designated by the *small interior box* and *horizontal line*, respectively. Error (*large box*) is S.E., *whiskers* represent the maximum and minimum values, and *asterisks* indicate $p < 0.05$ *versus* pH 7.6 via analysis of variance. *C*, schematic of NHX-7 protein: domain organization and Ca^{2+} regulatory motifs. Transmembrane domains are labeled with *Roman numerals*. Relevant *nhx-7* mutant alleles are listed in *italics*, with their positions denoted by *arrows*. *ok583* is a deletion allele that acts as a null, whereas *n2568* and *ox10* result in truncated proteins. Motifs targeted for mutagenesis were based upon homology with rat NHE1 (supplemental Fig. S1) and are denoted as well. The E271Q pore mutation is indicated by an *asterisk* in transmembrane domain VII. Other targets are marked schematically and by amino acid location within the *nhx-7* C-terminal coding sequence, including CHP, PIP_2, and CBD motifs and the single potential CaMKII phosphorylation site at Thr-618. Fusions between the N terminus of NHX-7 and the C terminus of other Na^+/H^+ exchangers occur in a conserved sequence in transmembrane domain XII.

Imaging Fluorescent Biosensors in C. elegans—Transgenic nematodes were imaged live and unrestrained as described previously (18). Imaging was performed with a 10× Nikon Plan Apo objective. Illumination was provided by a Polychrome IV monochromator (TILL Photonics) rigged to a Nikon Eclipse TE2000-S inverted microscope equipped with a high-speed charge-coupled device camera (Cooke). TILLvisION software was used for analysis, data were compiled in Microsoft Excel, and graphs were generated using Origin.

Measurements of Na^+/H^+ Exchange Activity in AP-1 Cells—AP-1 cells were cultured as described (48) and transfected using Lipofectamine LTX reagent (Invitrogen). After 24 h, cells were made quiescent by placing them in low-serum medium for at least 1 h. The cells were then loaded with the pH-sensitive fluorescent dye 2′,7′-bi-(2-carboxyethyl)-5(6)-carboxyfluorescein acetoxymethyl ester (Molecular Probes) and superfused with physiologic saline on a Nikon/TILL Photonics fluorescent imaging rig (described above), and incubation with high K^+/nigericin at varying pH values was used to calibrate the sensor (49). To measure Na^+/H^+ exchange activity, an ammonium prepulse was employed as described (48).

Confocal Microscopy—Confocal micrographs were obtained on an Olympus IX81 inverted laser scanning confocal microscope. The same parameters were used for all of the mutants when imaging across worm strains or across transfections.

Immunocytochemistry—Recombinant NHX-7 was detected using a mouse anti-V5 monoclonal antibody (1:2000; Invitrogen) and an Alexa Fluor 488-labeled goat anti-mouse secondary antibody (1:5000; Molecular Probes) using standard techniques.

CaM Binding Assay—In vitro transcription/translation (TNT; Promega) of linearized template DNA was used to label fusion proteins with [^{35}S]methionine. Proteins associating with biotinylated bovine CaM (5 μM; Calbiochem) were precipitated with streptavidin-agarose. Equivalent fractions of the starting and bound material were resolved by SDS-PAGE and visualized using autoradiography.

RNAi Treatment and DMP Assay—Nematodes were grown on bacteria expressing double-stranded RNA as described (50). Execution of the DMP was visualized under a dissecting microscope, and timing data were collected using Etho software, a keystroke recorder (51).

RESULTS

Recombinant NHX-7 Is an Authentic Na^+/H^+ Exchanger—To analyze NHX-7 exchange activity, a cDNA was expressed in AP-1 cells, a mammalian cell line that lacks endogenous Na^+/H^+ exchanger activity (31). Antibody staining of a V5 epitope tag built into the C terminus of NHX-7 confirmed its expression at the plasma membrane (see Fig. 3*F*). As is commonly observed with overexpression, some of the protein was retained in the endoplasmic reticulum as well. To test whether or not the exchanger was active, an ammonium prepulse was used to acidify the cells (52), and the rate of Na^+-dependent pH recovery was then measured. Eliciting NHX-7 activity from transfected cells required that they be starved of serum and that the measurements be performed within 24 h of transfection. Robust activity was observed, although the calculated exchange rate of NHX-7 was slower than that of the ubiquitous mammalian exchanger NHE1 (Fig. 1*A*). The NHX-7 exchange rate was sensitive to extracellular pH (pH_e) (Fig. 1*B*) and Na^+ ($K_m \sim 35$ mM). Surprisingly, agonists that raised intracellular Ca^{2+} levels had no significant effect on recombinant NHX-7 activity (data not shown).

Downloaded from http://www.jbc.org/ at University of Rochester on June 17, 2013

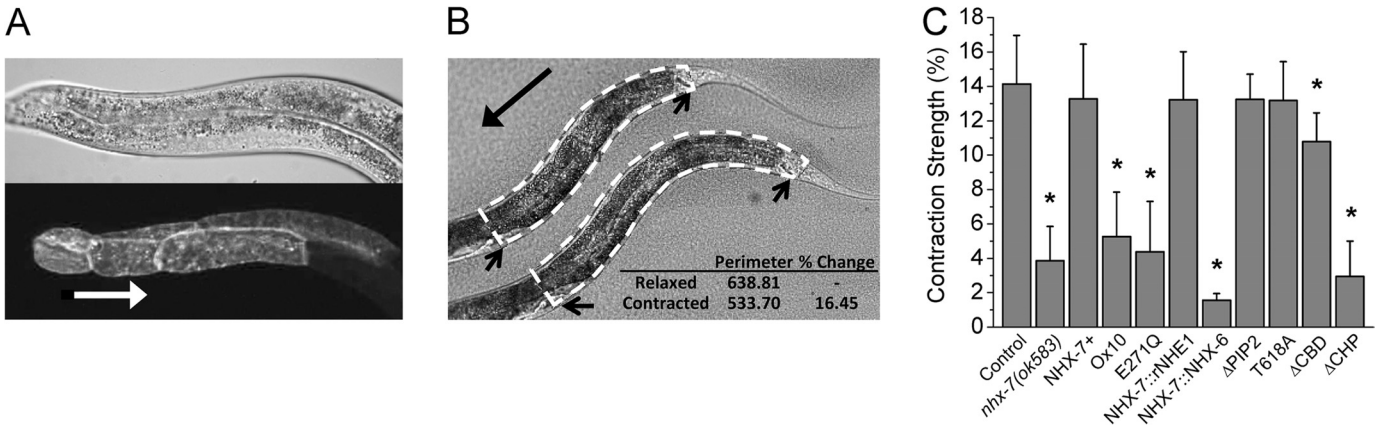

FIGURE 2. ***In vivo* structure-function analysis of NHX-7.** A transgenic construct coding for an *nhx-7* minigene fused to a cDNA for the red fluorescent protein mCherry was mutated at potential Ca^{2+} regulatory motifs or replaced with a homologous region from rNHE1 or NHX-6. The ability of these constructs to restore pBoc strength in an *nhx-7(ok585)* null mutant was assessed. *A*, confocal micrograph of p*nhx-7*::NHX-7::mCherry rescue construct expression in intestinal rings 7–9 (*lower*) and differential interference contrast (DIC) (*upper*). The *white arrow* points from posterior to anterior and is scaled to 50 μm. *B*, representative contraction assay using perimeter analysis. Values were calculated post hoc from a DIC video by measuring the perimeter (*dashed lines*) of the worm at both maximal relaxation (*lower*) and contraction (*upper*). *Arrows* indicate the vulva and anus, which were used as anterior and posterior reference points, respectively. An example calculation is shown in the *inset*. *C*, mutant pBoc strength. Transgenic constructs are denoted as follows: NHX-7+ is the WT transgene; *ox10* recapitulates a loss-of-function mutation identified through a forward genetic screen (deletion/frameshift starting approximately A702); E271Q is a pore mutation; NHX-7::rNHE1 and NHX-7::NHX-6 are fusions between the transmembrane domain of NHX-7 and the cytoplasmic domain of the indicated NHEs; ΔPIP_2 is a mutation of the PIP_2-binding site (K569A/K570A); T618A is a mutation of a CaMKII recognition site; ΔCBD is a deletion of the CBD from amino acids 695 to 723; ΔCHP is a mutation of the PBO-1-binding site (amino acids 541–545, MVQHL to RRQHR). Error is S.D. for between 7 and 27 worms per strain. *Asterisks* denote $p < 0.05$ *versus* the wild-type control via analysis of variance.

TABLE 1

Characteristics of *in vivo* NHX-7 mutagenesis

Shown below are the relative acidification rates and pBoc strength and duration in transgenic worms expressing mutant versions of NHX-7. pBoc duration values were derived post hoc from DIC videos. *pbo-5* mutants lack pBoc, but NHX-7 activity is identical to wild-type controls. The *nhx-7*(*ok583*) mutant strains expressing rescue constructs also contained the *pha-1* and *him-5* mutant alleles. Error is S.D. for contraction strength and duration and S.E. for acidification rate. The *n* value for each trial is shown in parentheses. ND, not determined.

Genetic background	Rescuing construct	Activity	Contraction strength	Contraction duration
		%	%	s
pbo-5 (n2303)		100 ± 10 (3)	ND	ND
pha-1(2123ts)/him-5(e1490)		ND	14.1 ± 2.8 (13)	4.1 ± 0.8 (13)
nhx-7(ok583)		20 ± 1 (3)[a]	3.9 ± 2.0 (17)[a]	3.1 ± 0.8 (16)[a]
nhx-7(ok583)	NHX-7+	120 ± 10 (3)	13.3 ± 3.2 (7)	5.0 ± 1.0 (7)
nhx-7(ok583)	*ox10*	26 ± 4 (3)[a]	5.7 ± 4.2 (27)[a]	3.3 ± 1.1 (24)
nhx-7(ok583)	E271Q	14 ± 2 (3)[a]	4.4 ± 2.9 (11)[a]	2.6 ± 0.3 (9)[a]
nhx-7(ok583)	NHX-7::rNHE1	67 ± 9 (3)	13.2 ± 2.8 (12)	3.8 ± 0.7 (12)
nhx-7(ok583)	NHX-7::NHX-6	26 ± 4 (3)[a]	1.6 ± 0.4 (8)[a]	1.1 ± 0.2 (5)[a]
nhx-7(ok583)	ΔPIP_2	31 ± 6 (3)[a]	13.2 ± 1.5 (10)	3.4 ± 0.4 (10)
nhx-7(ok583)	T618A	110 ± 20 (3)	13.3 ± 1.8 (11)	5.7 ± 0.5 (11)[a]
nhx-7(ok583)	ΔCBD	50 ± 4 (3)[a]	10.8 ± 1.7 (8)[a]	3.4 ± 0.3 (9)
nhx-7(ok583)	ΔCHP	ND	3.0 ± 2.1 (10)[a]	3.0 ± 0.3 (10)[a]
nhx-7(ok583)	rNHE1	30 ± 5 (3)[a]	4.3 ± 1.7 (9)[a]	3.9 ± 0.7 (4)

[a] $p < 0.05$ *versus* the NHX-7+ control via analysis of variance.

NHX-7 Is Regulated Similarly to Mammalian NHEs—As an alternative approach to AP-1 cells, we turned to an *in vivo* model to test whether Ca^{2+} regulates NHX-7. First, the ability of recombinant NHX-7 to complement a *C. elegans nhx-7(ok585)* loss-of-function mutant was tested. An mCherry fusion to NHX-7 (Fig. 2*A*) rescued the pBoc deficit in the mutant (Fig. 2*C* and Table 1), consistent with previous observations regarding an NHX-7::GFP fusion protein (18). The specificity of rescue was suggested by two observations: recapitulating an *nhx-7(ox10)* loss-of-function mutation that arises from a deletion/frameshift starting at about A702 suppressed the ability to restore pBoc, as did mutation of a critical amino acid residue in the pore region (E271Q) that is essential for Na^+/H^+ exchange activity (Fig. 2*C*).

NHX-7 has several motifs for input by Ca^{2+} signaling (Fig. 1*C*), which are shared with mammalian NHE1 in its C-terminal "regulatory domain" (supplemental Fig. S1). These shared motifs are likely to be functionally sufficient for coordinating upstream signaling, as the C-terminal coding sequence of rat NHE1 (rNHE1) effectively substituted for that of NHX-7 in the rescue construct (Fig. 2*C*). Conversely, a similar domain swap between NHX-7 and NHX-6, a worm exchanger that is coexpressed with NHX-7 in the intestine (41) but lacks notable homologous motifs for input by Ca^{2+} signaling (supplemental Fig. S1), did not rescue the mutant (Fig. 2*C*). However, NHE1 could not fully substitute for NHX-7, suggesting that there is some innate property of NHX-7 outside of the C terminus that strongly influences its ability to effectively function, through promoting proper localization, association with another protein(s), or transport activity itself.

Mutation of Putative Motifs for Ca^{2+} Regulation of NHX-7—Conserved potential Ca^{2+} regulatory motifs in NHX-7 (Fig. 1*C*)

Downloaded from http://www.jbc.org/ at University of Rochester on June 17, 2013

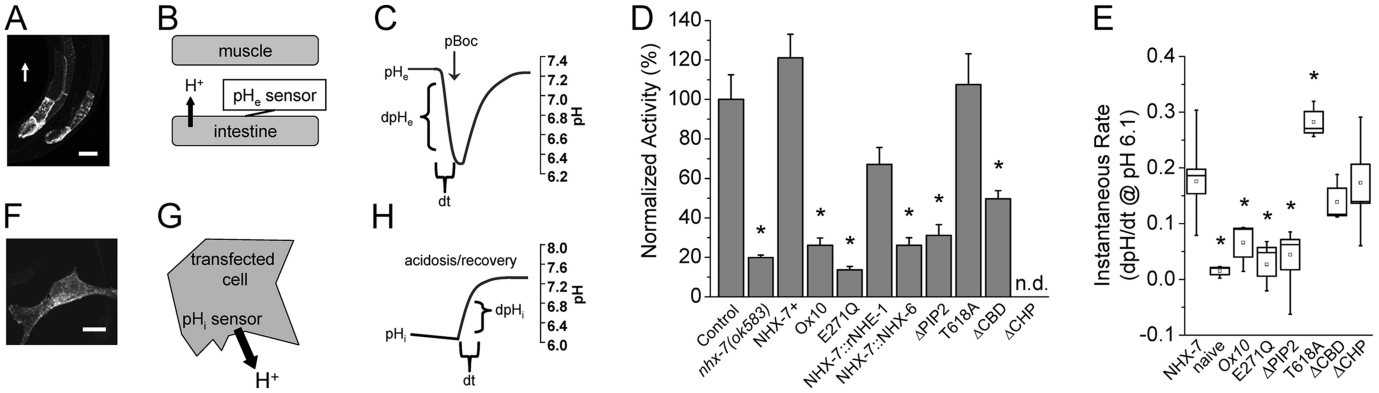

FIGURE 3. **Analysis of *in vivo*/*in vitro* exchanger activity.** A genetically encoded fluorescent pH sensor was targeted to the extracellular side of the posterior intestinal basolateral membrane to measure regional changes in pseudocoelomic pH during defecation in transgenic strains expressing WT and mutant *nhx-7* minigenes. To measure the basal activity of recombinant proteins, pH_i was monitored in transfected AP-1 cells in culture, and the rate of Na^+-dependent pH recovery following acidification was calculated. *A*, confocal micrograph of transgenic worms expressing the extracellular pH sensor at the basolateral membrane of intestinal rings 7–9. The *white arrow* denotes posterior-to-anterior orientation of the worm and is scaled to 50 μm. *B*, schematic of the extracellular pH sensor with protons moving from the intestine into the space between cells. *C*, representative trace of extracellular (pseudocoelomic) pH fluctuations that occur between the intestine and body wall muscle relative to pBoc. Dynamic fluorescent measurements of pH_e in freely moving worms were used to calculate the initial rate of acidification (dpH/d*t*), which is a function of NHX-7 activity. *D*, extracellular acidification rates resulting from expression of the mutant constructs are represented as normalized to the control strain. The resting pH of the pseudocoelom was not significantly different between strains, and the overall extent of acidification was proportional to the initial rate of acidification. Error is S.E. for three independent trials, with more than five worms per trial. *Asterisks* indicate $p < 0.05$ compared with the wild-type control via analysis of variance. *E*, instantaneous Na^+/H^+ exchange rate data for mutant NHX-7 constructs expressed in AP-1 cells *in vitro*. To calculate instantaneous recovery rate data, a best line fit equation was calculated for a 1-min window following the re-addition of Na^+ of a plot of dpH_i/dt *versus* pH and extrapolated to pH 6.1. Values were obtained from between three and nine independent experiments, with >10 cells imaged per experiment. The mean and median are designated by the *small interior box* and *horizontal line*, respectively. Error (*large box*) is S.E., *whiskers* represent the maximum and minimum values, and *asterisks* indicate $p < 0.05$ compared with cells expressing the wild-type NHX-7 via analysis of variance. *F*, confocal micrograph of an AP-1 cell expressing recombinant V5 epitope-tagged NHX-7 that has been visualized using anti-V5 primary and fluorescent Alexa Fluor 488-conjugated anti-mouse secondary antibodies. *Scale bar* = 10 μm. *G*, schematic of pH_i measurements in cell culture with protons moving out of the cell into the medium. *H*, representative trace of pH_i during Na^+-dependent pH recovery following acidification. The recovery rate was calculated based upon a plot of dpH_i/dt *versus* pH_i, with a best fit line extrapolated to pH 6.1.

were individually mutated, and the mutant constructs were tested for their ability to complement the loss-of-function mutant. These motifs included 1) a CaM-binding site of the 1-5-8-14 class, 2) a site for PIP_2 binding, 3) a CaMKII phosphorylation site, and 4) a binding site for the *C. elegans* CHP ortholog PBO-1 (54). Although there are other potential sites for Ca^{2+} regulation, these four sites represented the most likely candidates for the following reasons. First, the nonfunctional protein coded for by the *nhx-7(ox10)* allele has been shown to be truncated immediately prior to the start of the potential CaM-binding domain (CBD), suggesting that CaM binding might be import for NHX-7 function (17). Second, PIP_2 is a necessary cofactor for a variety of plasma membrane transporters, including NHEs (55), and during defecation, reductions in PIP_2 have been shown to activate TRPM channels, hence coordinating their activity with phospholipase C-mediated inositol trisphosphate production (56). Third, CHP is a cofactor for NHEs that has been suggested to mediate Ca^{2+} regulation of the exchanger (57, 58), and a *pbo-1* loss-of-function mutant lacks pBoc (54). Finally, phosphoregulation by CaMKII of a conserved site in NHE1 increases its activity in response to Ca^{2+} signaling (59, 60).

We were initially quite surprised to find that all of the mutant constructs supported robust pBoc (data not shown), at least until we considered that the mutant transgenes were being overexpressed and that overexpression could conceivably circumvent endogenous regulatory mechanisms. Hence, we established strains that approximated the wild-type expression levels of *nhx-7* as judged by quantitative RT-PCR (data not shown). Within this context, the PIP_2-binding site (ΔPIP_2) and CaMKII (T618A) mutants still rescued pBoc completely, but deletion of the CBD (ΔCBD) or CHP-binding sites (ΔCHP) reduced pBoc strength (Fig. 2*C*). The ΔCBD mutation resulted in a small but significant decrease in pBoc strength, whereas the ΔCHP mutation suppressed the ability of the transgene to rescue pBoc entirely (Table 1). Confocal microscopy was used to establish the abundance and membrane localization of the fluorescent mCherry-tagged NHX-7 mutant proteins, and whereas most of the mutants were indistinguishable from wild-type NHX-7::mCherry (data not shown), the ΔCHP protein accumulated at intracellular locations rather than at the basolateral membrane.[3]

We next considered the idea that the strength of pBoc may not directly reflect NHX-7 activity. pBoc is triggered by activation of proton receptors, whose pK_a is ~6.8 (17), on the body wall muscle cells, but proton extrusion, receptor activation, muscle response, and proton clearance mechanisms all likely impact the overall signaling output. Therefore, it seemed possible that reduction of NHX-7 activity could result in compensation from these other mechanisms or perhaps that NHX-7 normally extrudes an abundance of protons above and beyond that necessary for a normal behavioral response. If that were the case, then reductions in NHX-7 activity might be tolerated without a corresponding reduction in contraction strength.

We surmised that measuring changes in pH_e directly might be more informative regarding the mutations' effects on NHX-7 activity. To accomplish this, an extracellular pH bio-

[3] E. Allman and K. Nehrke, unpublished data.

Downloaded from http://www.jbc.org/ at University of Rochester on June 17, 2013

sensor (47) was expressed in the posterior intestinal cells and directed to the basolateral membrane (Fig. 3, *A* and *B*). In agreement with previous results (18), we were able to detect a transient robust acidification of the extracellular space between the posterior intestine and the overlying body wall muscle during pBoc in live moving worms (Fig. 3*C*). The observed acidification was largely absent in *nhx-7(ok583)* mutant worms, and measurements made in a *pbo-5(n2303)* background, which lacks the proton receptor and pBoc, suggested that the signal was not influenced by muscle contractility (Table 1). We then assessed the effect of each mutation on pH_e fluctuations and extended this analysis to include strains expressing the chimeric fusions with NHX-6 and rNHE1 described above (Fig. 3*D* and Table 1).

Our results suggest that three distinct categories of mutant phenotypes exist. There are mutants that support normal pH oscillations and rescue pBoc, mutants that have reduced exchange activity but still rescue pBoc, and mutants with little or no exchange activity and do not rescue pBoc. This last class mimics the *nhx-7(ok583)* null mutant. These results are consistent with our hypothesis that a reduction in NHX-7 activity can be tolerated without causing a visible phenotype. For example, the ΔCBD, ΔPIP_2, and chimeric rNHE1 proteins all rescued pBoc at least to some extent, but pH_e measurements suggested that they are less active than wild-type NHX-7 (Fig. 3*D*). In contrast, the NHX-6 chimera, ΔCHP mutant, *ox10* mutant, and E271Q pore mutant resembled the null mutant and exhibited low-amplitude pH oscillations that were unable to invoke contractions. The residual oscillations observed in the null mutant are likely due to the activities of other pH homeostatic mechanisms responding to intracellular acidification and causing some low level of proton efflux into the pseudocoelom. Finally, we note that the T618A mutation of the putative CaMKII phosphorylation site appears to have increased the activity of NHX-7, resulting in a strong contraction that was extended in duration (Table 1).

To directly assess whether the reduced activity observed with several of the mutants might be due to a reduction in basal levels of transport rather than disruption of Ca^{2+} signaling input, these mutants were expressed in AP-1 cells, and their transport rates were measured under quiescent conditions (Fig. 3, *E–H*). Approximately equal levels of NHX-7 expression and residence at the plasma membrane for each of the mutant proteins were suggested by immunolabeling and confocal microscopy (data not shown). Surprisingly, unlike our single-copy gene worm model, we found that enough of the ΔCHP mutant was trafficked to the cell surface in AP-1 cells to permit Na^+/H^+ exchange activity at similar levels as wild-type NHX-7 (Fig. 3*E*). Thus, the inability of the ΔCHP mutant to trigger pBoc was not due to it lacking transport activity. Similarly, the reduced activity of the ΔCBD mutant observed in worms was not a secondary consequence of reduced basal transport capacity (Fig. 3*E*). On the other hand, the enhanced activity of the T618A mutant in worms was recapitulated in AP-1 cells (Fig. 3*E*), suggesting that phosphorylation at Thr-618 by CaMKII may normally suppress basal activity. We also found that the ΔPIP_2 mutant, which had greatly reduced activity in worms but was able to support a nearly normal pBoc, did not function at all

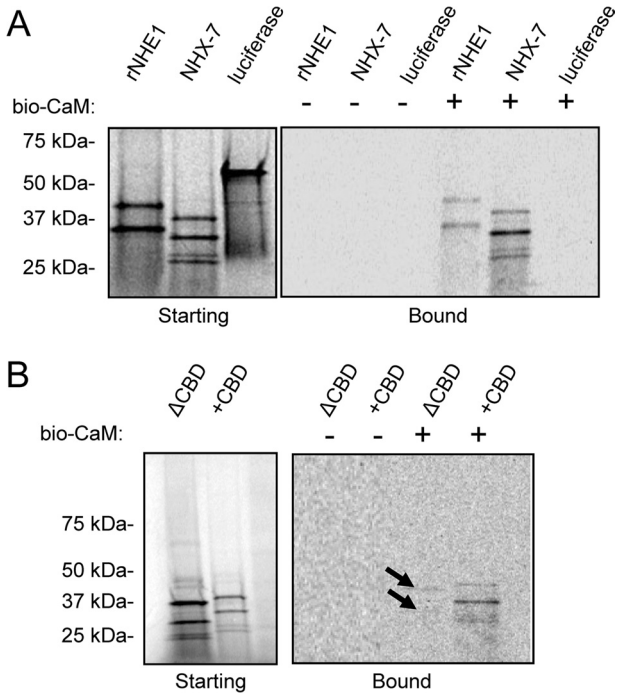

FIGURE 4. **Analysis of *in vitro* calmodulin binding by NHX-7.** The cytoplasmic C termini of both NHX-7 and rNHE1 were expressed *in vitro* as radiolabeled proteins, and their ability to bind to biotinylated bovine calmodulin (*bio-CaM*; 98% identical to worm CMD-1) was assessed by streptavidin fractionation, gel electrophoresis of the starting and bound fractions, and autoradiographic detection. *A*, autoradiograms of gel-fractionated ^{35}S-labeled proteins. The starting products from *in vitro* transcription/translation reactions (*left*) and bound fractions (*right*) are shown. An equivalent fraction of each was analyzed. Luciferase was used as a negative control. Multiple products are likely due to the use of PCR-amplified templates for *in vitro* transcription and do not interfere with the conclusion. Predicted molecular masses are as follows: rNHE1, ~36 kDa; NHX-7, ~31 kDa; and luciferase, 61 kDa. *B*, the CBD (identical to ΔCBD) was deleted, and the ability of the mutant ΔCBD protein to bind CaM was assessed as described above. *Arrows* denote slight residual CaM binding. The predicted molecular mass of ΔCBD is ~28 kDa.

in AP-1 cells (Fig. 3*E*). This could conceivably be due to higher levels of PIP_2 in worms *versus* cells in culture compensating for reduced PIP_2 binding affinity in the mutated exchanger, but it is also possible that Ca^{2+} activation in worms overcomes the observed reduced basal activity. Regardless, this result is inconsistent with the idea that reductions in PIP_2 might activate NHX-7 such as they do TRPM channels during defecation (56).

NHX-7/Calmodulin Binding and Knockdown of cmd-1, a Nematode Calmodulin Gene—The results of our mutagenesis suggested that CaM binding contributes to NHX-7 proton signaling during defecation. To test this more directly, an NHX-7 C-terminal protein fragment was labeled with [^{35}S]Met via *in vitro* transcription/translation, and the ability of the labeled protein to associate with biotinylated CaM was assessed by coprecipitation. NHE1, which is known to bind CaM (61), was used as a positive control to validate the assay (Fig. 4*A*). CaM associated with the soluble cytoplasmic C terminus of NHX-7 but did not associate with luciferase, which was used as a negative control (Fig. 4*A*). We also found that the K_d for CaM was similar to that for NHE1 (~8 nM) (data not shown). To confirm the specificity of this interaction, we demonstrated that the ΔCBD mutation significantly reduced CaM binding to NHX-7 (Fig. 4*B*).

Downloaded from http://www.jbc.org/ at University of Rochester on June 17, 2013

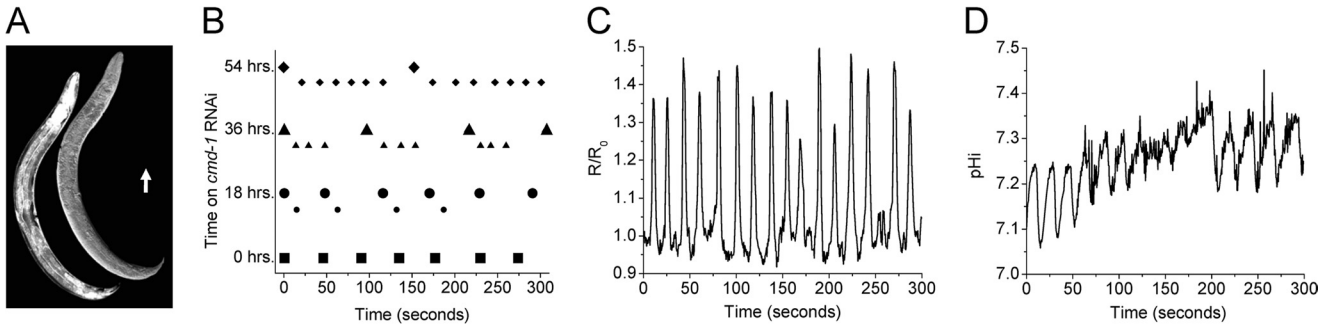

FIGURE 5. **The calmodulin gene *cmd-1* is required for normal defecation signaling.** RNAi was used to reduce *cmd-1* expression specifically in the intestine. Worms were placed onto *cmd-1* or control RNAi plates as L3 larva, and measurements were made following 0, 18, 36, and 54 h of RNAi. The fluorescent biosensors D3cpv and pHluorin were used to follow intestinal Ca^{2+} and pH_i oscillations, respectively, as *cmd-1* expression was reduced over time. *A*, composite image of a transgenic worm expressing a transcriptional fusion of the *cmd-1* promoter and the fluorescent protein mCherry (*left*) and the corresponding DIC image (*right*). The *arrow* indicates posterior-to-anterior orientation and is scaled to 50 μm. *B*, dot plots representing pBoc timing in individual worms following exposure to *cmd-1* RNAi for the time periods indicated (0, 18, 36, and 54 h). Strong contractions are plotted as *symbols*, whereas shadows or weak reiterative contractions are plotted as *smaller symbols* of like type placed lower on the *y axis*. *C*, representative Ca^{2+} oscillations in a *cmd-1* RNAi worm at 54 h. The oscillatory period shown here is similar to that of the behavioral reiterations shown in *B*. *D*, representative intestinal pH_i oscillations in a *cmd-1* RNAi worm at 54 h. Note that this trace represents fluctuations in pH_i rather than pH_e and that the period is similar to that of both Ca^{2+} oscillations and pBoc.

Having confirmed CaM binding and its physiologic relevance to NHX-7 function, we next asked whether reducing CaM levels *in vivo* would phenocopy the effect of the ΔCBD mutant on pBoc. The *C. elegans* genome contains five genes that encode Ca^{2+}-binding CaM-like proteins. The *cmd-1* gene codes for a nematode CaM ortholog that is 100% conserved with human CALM3. A transcriptional fusion between the *cmd-1* promoter and the red fluorescent protein mCherry coding sequence was broadly expressed in multiple cells and cell types, including body wall muscle, hypodermal cells, neurons, and, most relevant to our work, posterior intestinal cells (Fig. 5*A*). Therefore, the functional role of *cmd-1* was queried using RNAi-mediated knockdown. Unfortunately, global RNAi screens have shown that *cmd-1* is necessary for viability, and worms treated with *cmd-1* RNAi for several days died (data not shown). To circumvent this limitation, we turned to cell-specific RNAi. The RDE-1 protein is required for effective RNAi to occur, and an *rde-1* mutant strain can be complemented with a transgene expressing recombinant RDE-1 in a limited set of cells such as the intestine (25).

Here, we found that intestinal RNAi of *cmd-1* resulted in a progressive phenotype in which the cumulative loss of *cmd-1* expression altered defecation frequency (Fig. 5*B*). In general, when young adult worms were subjected to *cmd-1* RNAi for 18 h, they began to exhibit weak reiterations of the DMP. This has been observed previously in *unc-43* CaMKII loss-of-function mutants (20, 25), where these reiterations were referred to as "shadows" or "echos." The interval between the principal, or strong, DMP and the shadows was much shorter (~16–18 s) in *cmd-1* RNAi worms than the average defecation period (~45 s), consistent with *cmd-1* normally functioning to suppress inappropriate intracycle execution of the DMP. Surprisingly, however, an increased time of exposure to *cmd-1* RNAi resulted in not just a single shadow occurring after the principal DMP, but multiple shadows occurring (Fig. 5*B*). The period between principal executions of the DMP increased with loss of *cmd-1* primarily due to an increased number of shadows occurring between cycles, whereas the period between shadows, which was ~18 s, did not increase correspondingly. Eventually, the weaker shadows became nearly indistinguishable from the principal DMP. At this point, the worms were essentially defecating every ~18 s (Fig. 5). Continued exposure to *cmd-1* RNAi led to the cessation of defecation entirely, followed by death of the animal (data not shown).

Given that the DMP is initiated by oscillatory Ca^{2+} signaling and cyclic acidification of the intestine, we used fluorescent biosensors to measure Ca^{2+} and pH in the intestines of live moving worms subjected to *cmd-1* RNAi. Following 54 h, we observed oscillations in both of these second messengers occurring every ~18 s, mirroring the observed changes to the behavioral period (Fig. 5, *C* and *D*). We conclude that CaM directly influences intestinal oscillatory Ca^{2+} signaling upstream of acidification, and hence, its loss has effects that preclude analysis of its role in regulating NHX-7 directly. Nevertheless, these results are interesting in the context of signaling pathways that regulate the periodicity of Ca^{2+} oscillations and emphasize the integration between Ca^{2+} and proton signaling during defecation in worms.

DISCUSSION

Na^+/H^+ exchangers are recognized to contribute to pH_i homeostasis and electrolyte and water balance (for review, see Ref. 62). Recently, a new role for Na^+/H^+ exchangers has emerged from work in *C. elegans* showing that NHX-7 allows adjacent cells to communicate through direct proton signaling (17, 18). This event is coordinated by oscillatory Ca^{2+} signaling, which in turn leads to repetitive cellular acidification and recovery. Hence, defecation represents a behavior whose physiologic output is integrated by cross-talk between Ca^{2+} and pH signals. Counterintuitively, apart from its role in signaling, NHX-7 contributes little to re-establishing pH homeostasis following defecation. Because Na^+/H^+ exchangers are activated by allosteric proton binding and have been shown to be regulated by Ca^{2+}, it is reasonable to ask whether regulation of NHX-7 by Ca^{2+} is a determining factor in its ability to function as a signaling protein as opposed to a "pH housekeeper."

Apart from a relative insensitivity to the amiloride derivative 5-(*N*-ethyl-*N*-isopropyl)amiloride, NHX-7 functions much like mammalian NHEs and can facilitate recovery from induced acidosis when transfected into cells in culture (Fig. 1). However,

Downloaded from http://www.jbc.org/ at University of Rochester on June 17, 2013

initial attempts to discern the signaling pathway through which Ca^{2+} might stimulate NHX-7 were hampered by the fact that recombinant NHX-7 activity was not responsive to pharmacologic manipulations that increased intracellular Ca^{2+} levels. Although we considered the possibility that NHX-7 is not stimulated by Ca^{2+} signaling, we feel that it is more likely either that the relevant signaling pathway is not present in AP-1 cells or that it does not recognize the worm signaling motifs. Similarly, it is possible that overexpression in cell culture could mask Ca^{2+} regulatory effects on NHX-7.

Nevertheless, these simple observations helped to inform us as to how NHX-7 may contribute to the integrative physiology of defecation. In the worm, protons are an important means of performing work, and a proton gradient formed between the intestinal lumen and cell is essential for nutrient uptake across the apical membrane (50, 63). Maintenance of this gradient is critical and presents some physiologic challenges given that a significant portion of the intestine's luminal contents are expulsed every 45 s. To prevent their loss during expulsion, protons enter the cell from the lumen during defecation. These protons must then be quickly returned to the lumen immediately following defecation to drive nutrient uptake. Viewed in this context, sustained H^+ efflux through NHX-7 on the basolateral membrane could be catastrophic, leading to both caloric deprivation and systemic acidosis.

Our data demonstrate one mechanism for ensuring that proton efflux to the pseudocoelomic space via NHX-7 is acute. A brief pulse of activity is sufficient to rapidly acidify the small pseudocoelom to a nadir value at which we found NHX-7 was virtually inactive (Fig. 1*B*). Therefore, the inherent pH_e sensitivity of NHX-7 appears to provide a failsafe method of ensuring that H^+ signaling is turned off following stimulation of the muscle proton receptor.

A transgenic worm model allowed us to perform structure-function mutagenesis of NHX-7 and complementation of a null mutant to assess the role of potential Ca^{2+} regulatory motifs. Our results from both behavioral output and *in vivo* pH measurements taken together suggest that 1) PIP_2 binding stimulates basal NHX-7 activity, 2) CaM binding contributes to Ca^{2+} activation of NHX-7, and 3) stimulated NHX-7 activity exceeds what is necessary to trigger a "normal" pBoc. Binding of the CHP ortholog PBO-1 appears to affect NHX-7 trafficking and/or membrane residence through an unexplored mechanism (data not shown); hence, we were unable to define its role in Ca^{2+} activation, although given its EF-hand Ca^{2+}-binding domains, we hypothesize that it may serve dual roles in transport and signaling. We also found that a T618A mutation of a potential CaMKII phosphorylation site increased the duration of pBoc and the period of extracellular acidification during pBoc (Fig. 3 and Table 1). Although the effect of the T618A mutation was relatively modest, phosphorylation by CaMKII at this site may provide a "cellular memory" of Ca^{2+} signaling, such as occurs during long-term potentiation in neurons (64), hence contributing to feedback inhibition of NHE activity.

Interestingly, crystal structure data from bacterial NhaA and from a CHP/NHE1 fragment suggest a possible mechanism of action for CHP and PIP_2 whereby their binding near helical segment 11, which has been shown to be important for exchange activity, could have direct implications in the transport of ions (65, 66). Moreover, Ca^{2+} regulation of NHX-7 appears to be uncoupled from the primary regulation by H^+, consistent with the pH sensor responsible for H^+ recognition being located at the beginning of helix 9 on the opposite side of the unwound helix 11 (65).

Regulation by CaM is more difficult to interpret mechanistically, as its binding occurs farther downstream in the C-terminal tail, and the binding site(s) in NHX-7 and NHE1 are not precisely conserved at the linear sequence level (supplemental Fig. S1). Although CaM itself is not well studied in *C. elegans*, CaMKII has been studied extensively, and genetic approaches have shown that mutations in *unc-43*, the worm CaMKII ortholog, cause the DMP to be reiterated, albeit weakly (20). This ability of CaMKII to normally suppress inappropriate Ca^{2+} oscillations between cycles is consistent with cellular memory. We discovered that loss of CaM itself resulted in a qualitatively similar result (Fig. 5). However, we also discovered that this phenotype was progressive and that the strength and occurrence of these reiterations became more pronounced over time. Astoundingly, after several days of exposure to *cmd-1* RNAi, the worms were executing the entire DMP every ~18 s, and shortly thereafter, they expired.

To understand the physiologic alteration accompanying these shadow contractions, we also went on to show that late-stage *cmd-1* RNAi worms exhibited Ca^{2+} and pH oscillations at nearly three times the rate of normal worms (Fig. 5). At this rate, intestinal pH recovery processes, most likely those of the energy-dependent second-phase V-ATPase (63), can not accommodate the cyclic acidification that occurs, resulting in sustained cellular acidosis well below that of the normal resting pH at ~7.4 (Fig. 5*D*). We speculate that *cmd-1* may contribute to regulating the inositol 1,4,5-trisphosphate receptor ITR-1, which is the molecular pacemaker for defecation. Although we found these results to be noteworthy and to deserve reporting, the fact that *cmd-1* contributed to Ca^{2+} pacemaking and that its loss induced massive cellular acidification derailed our attempts to confirm CaM regulation of NHX-7 through *cmd-1* RNAi.

Considered as a whole, our data support a model in which Ca^{2+} activation of NHX-7 is not essential for its function but may contribute to proton conservation. Moreover, we have shown that PIP_2 binding is required for basal function of the exchanger and suggested that Ca^{2+} may also play a role in suppressing the activity of NHX-7 following its activation. Finally, although it appears likely that CaM helps to coordinate Ca^{2+} activation of NHX-7, it also regulates oscillatory Ca^{2+} signaling frequency upstream of NHX-7 activity.

In conclusion, the apparent sensitivity of NHX-7 within the integrative context of defecation to changes in both Ca^{2+} and pH is consistent with the importance that protons play in intestinal physiology in the worm but may also provide mechanistic insights into the regulation of NHE activity in mammals. For example, Na^+/H^+ exchange has been implicated in the regulation of synaptic transmission at glutamatergic, GABAergic, and dopaminergic synapses (67–69), and NHE1 has been shown to contribute to synaptic acidification and the creation of an acidic microdomain at the synaptic cleft (70). It is likely not coinci-

Downloaded from http://www.jbc.org/ at University of Rochester on June 17, 2013

dental that synaptic vesicle release is a Ca^{2+}-mediated event. Alternatively, NHE5 is credited with supporting neuronal activity-dependent dendritic spine growth through a novel pH-mediated negative feedback mechanism (53). These results suggest that acute control of pH and proton transport across the membrane has profound consequences for mammalian neurophysiology and may potentially affect communication between adjacent cells in a variety of contexts, including, as we have shown here, during signaling between intestinal and muscle cells in *C. elegans*.

Acknowledgments—We thank Teresa Sherman for technical assistance, Dr. L. Pablo Cid for the extracellular pH sensor, and Dr. Maureen Peters for critical comments. Some strains used in this work were provided by the C. elegans Gene Knockout Consortium and the Caenorhabditis Genetics Center, which is supported by National Institutes of Health Office of Research Infrastructure Program P40 OD010440.

REFERENCES

1. Casey, J. R., Grinstein, S., and Orlowski, J. (2010) Sensors and regulators of intracellular pH. *Nat. Rev. Mol. Cell Biol.* **11,** 50–61
2. Alper, S. L. (2002) Genetic diseases of acid-base transporters. *Annu. Rev. Physiol.* **64,** 899–923
3. Garbern, J. Y., Neumann, M., Trojanowski, J. Q., Lee, V. M., Feldman, G., Norris, J. W., Friez, M. J., Schwartz, C. E., Stevenson, R., and Sima, A. A. (2010) A mutation affecting the sodium/proton exchanger, SLC9A6, causes mental retardation with tau deposition. *Brain* **133,** 1391–1402
4. Martínez-Zaguilán, R., Seftor, E. A., Seftor, R. E., Chu, Y. W., Gillies, R. J., and Hendrix, M. J. (1996) Acidic pH enhances the invasive behavior of human melanoma cells. *Clin. Exp. Metastasis* **14,** 176–186
5. Ludwig, M. G., Vanek, M., Guerini, D., Gasser, J. A., Jones, C. E., Junker, U., Hofstetter, H., Wolf, R. M., and Seuwen, K. (2003) Proton-sensing G-protein-coupled receptors. *Nature* **425,** 93–98
6. Li, S., Sato, S., Yang, X., Preisig, P. A., and Alpern, R. J. (2004) Pyk2 activation is integral to acid stimulation of sodium/hydrogen exchanger 3. *J. Clin. Invest.* **114,** 1782–1789
7. Waldmann, R., Champigny, G., Bassilana, F., Heurteaux, C., and Lazdunski, M. (1997) A proton-gated cation channel involved in acid-sensing. *Nature* **386,** 173–177
8. Ishii, S., Kihara, Y., and Shimizu, T. (2005) Identification of T cell death-associated gene 8 (TDAG8) as a novel acid sensing G-protein-coupled receptor. *J. Biol. Chem.* **280,** 9083–9087
9. Tomura, H., Mogi, C., Sato, K., and Okajima, F. (2005) Proton-sensing and lysolipid-sensitive G-protein-coupled receptors: a novel type of multifunctional receptors. *Cell. Signal.* **17,** 1466–1476
10. Wemmie, J. A., Price, M. P., and Welsh, M. J. (2006) Acid-sensing ion channels: advances, questions and therapeutic opportunities. *Trends Neurosci.* **29,** 578–586
11. Dray, A. (1995) Inflammatory mediators of pain. *Br. J. Anaesth.* **75,** 125–131
12. Issberner, U., Reeh, P. W., and Steen, K. H. (1996) Pain due to tissue acidosis: a mechanism for inflammatory and ischemic myalgia? *Neurosci. Lett.* **208,** 191–194
13. Cobbe, S. M., and Poole-Wilson, P. A. (1980) The time of onset and severity of acidosis in myocardial ischaemia. *J. Mol. Cell. Cardiol.* **12,** 745–760
14. Chesler, M., and Kaila, K. (1992) Modulation of pH by neuronal activity. *Trends Neurosci.* **15,** 396–402
15. Krishtal, O. A., Osipchuk, Y. V., Shelest, T. N., and Smirnoff, S. V. (1987) Rapid extracellular pH transients related to synaptic transmission in rat hippocampal slices. *Brain Res.* **436,** 352–356
16. Vessey, J. P., Stratis, A. K., Daniels, B. A., Da Silva, N., Jonz, M. G., Lalonde, M. R., Baldridge, W. H., and Barnes, S. (2005) Proton-mediated feedback inhibition of presynaptic calcium channels at the cone photoreceptor synapse. *J. Neurosci.* **25,** 4108–4117
17. Beg, A. A., Ernstrom, G. G., Nix, P., Davis, M. W., and Jorgensen, E. M. (2008) Protons act as a transmitter for muscle contraction in *C. elegans*. *Cell* **132,** 149–160
18. Pfeiffer, J., Johnson, D., and Nehrke, K. (2008) Oscillatory transepithelial H^+ flux regulates a rhythmic behavior in *C. elegans*. *Curr. Biol.* **18,** 297–302
19. Thomas, J. H. (1990) Genetic analysis of defecation in *Caenorhabditis elegans*. *Genetics* **124,** 855–872
20. Liu, D. W., and Thomas, J. H. (1994) Regulation of a periodic motor program in *C. elegans*. *J. Neurosci.* **14,** 1953–1962
21. Croll, N. A., and Smith, J. M. (1978) Integrated behaviour in the feeding phase of *Caenorhabditis elegans* (Nematoda). *J. Zool.* **184,** 507–517
22. Dal Santo, P., Logan, M. A., Chisholm, A. D., and Jorgensen, E. M. (1999) The inositol triphosphate receptor regulates a 50-second behavioral rhythm in *C. elegans*. *Cell* **98,** 757–767
23. Espelt, M. V., Estevez, A. Y., Yin, X., and Strange, K. (2005) Oscillatory Ca^{2+} signaling in the isolated *Caenorhabditis elegans* intestine: role of the inositol-1,4,5-trisphosphate receptor and phospholipases C β and γ. *J. Gen. Physiol.* **126,** 379–392
24. Teramoto, T., and Iwasaki, K. (2006) Intestinal calcium waves coordinate a behavioral motor program in *C. elegans*. *Cell Calcium* **40,** 319–327
25. Nehrke, K., Denton, J., and Mowrey, W. (2008) Intestinal Ca^{2+} wave dynamics in freely moving *C. elegans* coordinate execution of a rhythmic motor program. *Am. J. Physiol. Cell Physiol.* **294,** C333–C344
26. Slepkov, E. R., Rainey, J. K., Sykes, B. D., and Fliegel, L. (2007) Structural and functional analysis of the Na^+/H^+ exchanger. *Biochem. J.* **401,** 623–633
27. Denker, S. P., and Barber, D. L. (2002) Cell migration requires both ion translocation and cytoskeletal anchoring by the Na-H exchanger NHE1. *J. Cell Biol.* **159,** 1087–1096
28. Pouysségur, J., Sardet, C., Franchi, A., L'Allemain, G., and Paris, S. (1984) A specific mutation abolishing Na^+/H^+ antiport activity in hamster fibroblasts precludes growth at neutral and acidic pH. *Proc. Natl. Acad. Sci. U.S.A.* **81,** 4833–4837
29. Putney, L. K., and Barber, D. L. (2003) Na-H exchange-dependent increase in intracellular pH times G_2/M entry and transition. *J. Biol. Chem.* **278,** 44645–44649
30. Tominaga, T., and Barber, D. L. (1998) Na-H exchange acts downstream of RhoA to regulate integrin-induced cell adhesion and spreading. *Mol. Biol. Cell* **9,** 2287–2303
31. Rotin, D., and Grinstein, S. (1989) Impaired cell volume regulation in Na^+-H+ exchange-deficient mutants. *Am. J. Physiol.* **257,** C1158–C1165
32. Rotin, D., Steele-Norwood, D., Grinstein, S., and Tannock, I. (1989) Requirement of the Na^+/H^+ exchanger for tumor growth. *Cancer Res.* **49,** 205–211
33. Sardet, C., Franchi, A., and Pouysségur, J. (1989) Molecular cloning, primary structure, and expression of the human growth factor-activatable Na^+/H^+ antiporter. *Cell* **56,** 271–280
34. Orlowski, J., Kandasamy, R. A., and Shull, G. E. (1992) Molecular cloning of putative members of the Na/H exchanger gene family. cDNA cloning, deduced amino acid sequence, and mRNA tissue expression of the rat Na/H exchanger NHE-1 and two structurally related proteins. *J. Biol. Chem.* **267,** 9331–9339
35. Wang, Z., Orlowski, J., and Shull, G. E. (1993) Primary structure and functional expression of a novel gastrointestinal isoform of the rat Na/H exchanger. *J. Biol. Chem.* **268,** 11925–11928
36. Numata, M., Petrecca, K., Lake, N., and Orlowski, J. (1998) Identification of a mitochondrial Na^+/H^+ exchanger. *J. Biol. Chem.* **273,** 6951–6959
37. Attaphitaya, S., Park, K., and Melvin, J. E. (1999) Molecular cloning and functional expression of a rat Na^+/H^+ exchanger (NHE5) highly expressed in brain. *J. Biol. Chem.* **274,** 4383–4388
38. Baird, N. R., Orlowski, J., Szabó, E. Z., Zaun, H. C., Schultheis, P. J., Menon, A. G., and Shull, G. E. (1999) Molecular cloning, genomic organization, and functional expression of Na^+/H^+ exchanger isoform 5 (NHE5) from human brain. *J. Biol. Chem.* **274,** 4377–4382
39. Goyal, S., Vanden Heuvel, G., and Aronson, P. S. (2003) Renal expression of novel Na^+/H^+ exchanger isoform NHE8. *Am. J. Physiol. Renal Physiol.*

Downloaded from http://www.jbc.org/ at University of Rochester on June 17, 2013

284, F467–E473
40. Nakamura, N., Tanaka, S., Teko, Y., Mitsui, K., and Kanazawa, H. (2005) Four Na^+/H^+ exchanger isoforms are distributed to Golgi and post-Golgi compartments and are involved in organelle pH regulation. *J. Biol. Chem.* **280,** 1561–1572
41. Nehrke, K., and Melvin, J. E. (2002) The NHX family of Na^+-H^+ exchangers in *Caenorhabditis elegans*. *J. Biol. Chem.* **277,** 29036–29044
42. Noël, J., and Pouysségur, J. (1995) Hormonal regulation, pharmacology, and membrane sorting of vertebrate Na^+/H^+ exchanger isoforms. *Am. J. Physiol.* **268,** C283–C296
43. Aronson, P. S., Nee, J., and Suhm, M. A. (1982) Modifier role of internal H^+ in activating the Na^+-H^+ exchanger in renal microvillus membrane vesicles. *Nature* **299,** 161–163
44. Imahashi, K., Mraiche, F., Steenbergen, C., Murphy, E., and Fliegel, L. (2007) Overexpression of the Na^+/H^+ exchanger and ischemia-reperfusion injury in the myocardium. *Am. J. Physiol. Heart Circ. Physiol.* **292,** H2237–H2247
45. He, P., and Yun, C. C. (2010) Mechanisms of the regulation of the intestinal Na^+/H^+ exchanger NHE3. *J. Biomed. Biotechnol.* **2010,** 238080
46. Brenner, S. (1974) The genetics of *Caenorhabditis elegans*. *Genetics* **77,** 71–94
47. Urra, J., Sandoval, M., Cornejo, I., Barros, L. F., Sepúlveda, F. V., and Cid, L. P. (2008) A genetically encoded ratiometric sensor to measure extracellular pH in microdomains bounded by basolateral membranes of epithelial cells. *Pflugers Arch.* **457,** 233–242
48. Johnson, D., Allman, E., and Nehrke, K. (2012) Regulation of acid-base transporters by reactive oxygen species following mitochondrial fragmentation. *Am. J. Physiol. Cell Physiol.* **302,** C1045–C1054
49. Thomas, J. A., Buchsbaum, R. N., Zimniak, A., and Racker, E. (1979) Intracellular pH measurements in Ehrlich ascites tumor cells utilizing spectroscopic probes generated *in situ*. *Biochemistry* **18,** 2210–2218
50. Nehrke, K. (2003) A reduction in intestinal cell pH_i due to loss of the *Caenorhabditis elegans* Na^+/H^+ exchanger NHX-2 increases life span. *J. Biol. Chem.* **278,** 44657–44666
51. Iwasaki, K., Liu, D. W., and Thomas, J. H. (1995) Genes that control a temperature-compensated ultradian clock in *Caenorhabditis elegans*. *Proc. Natl. Acad. Sci. U.S.A.* **92,** 10317–10321
52. Boron, W. F., and De Weer, P. (1976) Intracellular pH transients in squid giant axons caused by CO_2, NH_3, and metabolic inhibitors. *J. Gen. Physiol.* **67,** 91–112
53. Diering, G. H., Mills, F., Bamji, S. X., and Numata, M. (2011) Regulation of dendritic spine growth through activity-dependent recruitment of the brain-enriched Na^+/H^+ exchanger NHE5. *Mol. Biol. Cell* **22,** 2246–2257
54. Wagner, J., Allman, E., Taylor, A., Ulmschneider, K., Kovanda, T., Ulmschneider, B., Nehrke, K., and Peters, M. A. (2011) A calcineurin homologous protein is required for sodium-proton exchange events in the *C. elegans* intestine. *Am. J. Physiol. Cell Physiol.* **301,** C1389–C1403
55. Aharonovitz, O., Zaun, H. C., Balla, T., York, J. D., Orlowski, J., and Grinstein, S. (2000) Intracellular pH regulation by Na^+/H^+ exchange requires phosphatidylinositol 4,5-bisphosphate. *J. Cell Biol.* **150,** 213–224
56. Xing, J., and Strange, K. (2010) Phosphatidylinositol 4,5-bisphosphate and loss of PLCγ activity inhibit TRPM channels required for oscillatory Ca^{2+} signaling. *Am. J. Physiol. Cell Physiol.* **298,** C274–C282
57. Pang, T., Su, X., Wakabayashi, S., and Shigekawa, M. (2001) Calcineurin homologous protein as an essential cofactor for Na^+/H^+ exchangers. *J. Biol. Chem.* **276,** 17367–17372
58. Lin, X., and Barber, D. L. (1996) A calcineurin homologous protein inhibits GTPase-stimulated Na-H exchange. *Proc. Natl. Acad. Sci. U.S.A.* **93,** 12631–12636
59. Fliegel, L., Walsh, M. P., Singh, D., Wong, C., and Barr, A. (1992) Phosphorylation of the C-terminal domain of the Na^+/H^+ exchanger by Ca^{2+}/calmodulin-dependent protein kinase II. *Biochem. J.* **282,** 139–145
60. Vila-Petroff, M., Mundiña-Weilenmann, C., Lezcano, N., Snabaitis, A. K., Huergo, M. A., Valverde, C. A., Avkiran, M., and Mattiazzi, A. (2010) Ca^{2+}/calmodulin-dependent protein kinase II contributes to intracellular pH recovery from acidosis via Na^+/H^+ exchanger activation. *J. Mol. Cell. Cardiol.* **49,** 106–112
61. Bertrand, B., Wakabayashi, S., Ikeda, T., Pouysségur, J., and Shigekawa, M. (1994) The Na^+/H^+ exchanger isoform 1 (NHE1) is a novel member of the calmodulin-binding proteins. Identification and characterization of calmodulin-binding sites. *J. Biol. Chem.* **269,** 13703–13709
62. Putney, L. K., Denker, S. P., and Barber, D. L. (2002) The changing face of the Na^+/H^+ exchanger, NHE1: structure, regulation, and cellular actions. *Annu. Rev. Pharmacol. Toxicol.* **42,** 527–552
63. Allman, E., Johnson, D., and Nehrke, K. (2009) Loss of the apical V-ATPase a-subunit VHA-6 prevents acidification of the intestinal lumen during a rhythmic behavior in *C. elegans*. *Am. J. Physiol. Cell Physiol.* **297,** C1071–C1081
64. Lisman, J., Yasuda, R., and Raghavachari, S. (2012) Mechanisms of CaMKII action in long-term potentiation. *Nat. Rev. Neurosci.* **13,** 169–182
65. Hunte, C., Screpanti, E., Venturi, M., Rimon, A., Padan, E., and Michel, H. (2005) Structure of a Na^+/H^+ antiporter and insights into mechanism of action and regulation by pH. *Nature* **435,** 1197–1202
66. Mishima, M., Wakabayashi, S., and Kojima, C. (2007) Solution structure of the cytoplasmic region of Na^+/H^+ exchanger 1 complexed with essential cofactor calcineurin B homologous protein 1. *J. Biol. Chem.* **282,** 2741–2751
67. Trudeau, L. E., Parpura, V., and Haydon, P. G. (1999) Activation of neurotransmitter release in hippocampal nerve terminals during recovery from intracellular acidification. *J. Neurophysiol.* **81,** 2627–2635
68. Jang, I. S., Brodwick, M. S., Wang, Z. M., Jeong, H. J., Choi, B. J., and Akaike, N. (2006) The Na^+/H^+ exchanger is a major pH regulator in GABAergic presynaptic nerve terminals synapsing onto rat CA3 pyramidal neurons. *J. Neurochem.* **99,** 1224–1236
69. Rocha, M. A., Crockett, D. P., Wong, L. Y., Richardson, J. R., and Sonsalla, P. K. (2008) Na^+/H^+ exchanger inhibition modifies dopamine neurotransmission during normal and metabolic stress conditions. *J. Neurochem.* **106,** 231–243
70. Dietrich, C. J., and Morad, M. (2010) Synaptic acidification enhances $GABA_A$ signaling. *J. Neurosci.* **30,** 16044–16052

Downloaded from http://www.jbc.org/ at University of Rochester on June 17, 2013

References This article cites 70 articles, 38 of which you can access for free at:
http://www.jbc.org/content/288/8/5886#BIBL

Downloaded from http://www.jbc.org/ at University of Rochester on June 17, 2013